

**KINETIC ENERGY DISTRIBUTION OF H (2p) ATOMS FROM
DISSOCIATIVE EXCITATION OF H₂**

**JOSEPH M. AJELLO
SYED M. AHMED
ISIK KANIK
ROSALIE MULTARI**

**JET PROPULSION LABORATORY
CALIFORNIA INSTITUTE OF TECHNOLOGY
PASADENA, CALIFORNIA 91109**

**SUBMITTED TO :
PHYSICAL REVIEW LETTERS**

MARCH 1, 1995

ABSTRACT

The kinetic energy distribution of H(2p) atoms resulting from electron impact dissociation of H₂ has been measured by an ultraviolet (uv) spectroscopic technique. A high-resolution uv spectrometer was employed for the measurement of the H Lyman- α (H L α) emission line profile at 20 eV and 100 eV electron impact energies. Analysis of the deconvolved 100-eV line profile reveals the existence of a narrow line peak and a broad pedestal base. Slow H(2p) atoms with peak energy near 80 meV produce the peak profile, which is nearly independent of impact energy. The wings of H L α arise from dissociative excitation of a series of doubly excited Q, and Q₂ states, which define the core orbitals. The energy distribution of the fast atoms shows a peak at 4 eV.

PACS CLASSIFICATION: 34.80.Gs (ELECTRON SCATTERING - MOLECULAR DISSOCIATION), 33.50Dq (MOLECULAR SPECTRA - FLUORESCENCE)

INTRODUCTION

The kinetic distribution of H(2s) atoms from dissociative excitation of H₂ has been the subject of much published research¹⁻⁷, particularly in the late 1960's through 1980. The kinetic energy distribution function of H(2p) atoms from dissociative excitation of H₂ has not previously been measured. There are expected to be two distinct maxima in the kinetic energy distribution by analogy to results obtained from the distribution of H(2s) and H(nℓ) atoms, where n=3, 4 and 5. A comparison of the H(2p) and H(2s) distributions is of fundamental importance in understanding the dynamics of the H₂ dissociation process which can occur from singly excited or doubly excited states. The former lead to the "slow" component and the latter lead to the "fast" component. In the separated atom limit, non-adiabatic coupling of the nearly degenerate 2p and 2s states are expected to lead to cross-over of the H(2p) and H(2s) fragments.⁸ For higher principal quantum numbers through n=5, studies of H(nℓ) kinetic energy distribution function has been carried out for many years by Ogawa and coworkers.⁹⁻¹² Their interferometric technique involves measurement of the Doppler line profile of Balmer-α, -β, and -γ in the visible and near uv portion of the spectrum. The Balmer-α line profile at 6562.86 Å, for example, shows a characteristic narrow central peak (-300 mÅ FWHM) and a broad wing (-1.8 Å FWHM). In this work a spectroscopic technique was employed using a 3-meter high resolution vacuum ultraviolet (vuv) spectrometer to measure the line profile of H La at 1215.67 Å. Since the Doppler wavelength shift is proportional to the emission line wavelength, five to six times narrower line profiles can be expected in the vuv.

Most measurements of H(2s) kinetic energy distributions have been obtained by TOF techniques. The TOF spectra are complicated, in many cases, by the blending of signals from H(2s) metastable atoms and high Rydberg atoms. The threshold appearance potentials (AP) are frequently uncertain to ±1 eV or more. Great disparity exists with regard to the threshold for the fast H(2s) component compared to that of higher members of the Rydberg series. Misakian and Zorn¹ identified an AP at 29 eV for n=2. Spezeski et al.⁴ pointed out that the AP must be less than 27 eV, whereas Ogawa and Higo⁹ measured thresholds of 24 and 27 ± 1 eV for n=4. In this work, we clearly identify three separate AP to ± 0.5 eV accuracy for the fast H(2p) atoms.

Misakian and Zorn¹ placed the AP for slow H(2s) atoms at 14.9 ± 0.3 eV. Direct dissociation and predissociation as well as resonance and cascade processes can contribute to this threshold for H(2s) and H(2p). We have recently modeled the total absolute emission cross section of H La into six separate fast and slow processes from low resolution studies of the unresolved H La line.¹³ This work produces a direct measurement of

the fraction of fast atoms and supports our method of analysis of total emission cross sections.

EXPERIMENTAL

The experimental system has been described in a recent paper.⁴ In brief, it consists of a high-resolution 3-meter uv spectrometer in tandem with an electron impact collision chamber. A resolving power of 50,000 is achieved by operating the spectrometer in third order. The line shapes were measured with experimental conditions that ensure linearity of signal with electron beam current and gas pressure. All spectral and cross section data were obtained in the crossed beam mode. The line profiles were measured at 90° to the electron beam axis and molecular beam axis. The electron impact-induced fluorescent line profiles of H La at 20 and 100 eV impact energies are shown in Fig. 1, along with the instrument slit function. As expected, the line profiles consist of a narrow central peak and a broad wing base at 100 eV impact energy. The line profile at 20 eV shows no pedestal base structure. The H La line is actually a closely spaced multiplet (of) doublet structure. The 2P-_s multiplet may be weakly polarized depending on the magnetic sublevel population and/or the spatial distribution of dissociation products.¹⁵ We have acquired a vuv polarizer to complete this aspect of the study. In this study we assume the anisotropy is small. The measured FWHM of 47 mÅ and 49 mÅ for the 100 eV and 20 eV line profiles, respectively, are not narrow with respect to the instrumental slit function (FWHM = 24 mÅ). Fast Fourier Transform (FFT) techniques were used to recover the actual line profile.¹⁶ The measured line profile is the convolution of the true line profile and the instrumental slit function. The measured line profile, $I(\lambda)$ is given by the following convolution integral

$$I(\lambda) = \int T(\lambda') A(\lambda - \lambda') d\lambda', \quad (1)$$

where $T(\lambda')$ is the true line profile at wavelength λ' and $A(\lambda - \lambda')$ is the instrumental response function.

RESULTS

The kinetic energy distribution of the fragments, $P(E)$, is given by

$$P(E) = k(dT/d\lambda), \quad (2)$$

where k is a multiplicative constant.¹⁰ The kinetic distribution of the H(2p) fragments is shown in Fig. 2 for the slow fragment distribution and in Fig. 3 for the combined fast and slow fragment H(2p) distributions. The kinetic energy distribution is obtained by finding the true line profile, $T(\lambda)$, of H La from the FFT of eqn. 1. The deconvolved true line

\wedge
 $\wedge \wedge$
 profile of the central peak is found to have a FWHM of 40 ± 4 mÅ for both the 20 and 100 eV H L α line profiles. Figure 2 shows the slow fragment H(2p) kinetic energy distribution for both the 100 eV and 20 eV line profiles given in Fig. 1. Since the measured H L α line profile for the central peak at 100 eV is nearly identical to the 20 eV line profile, it follows that the resultant slow fragment distribution for each impact energy displays the same shape. The slow fragment distribution has a peak at 80 ± 10 meV and 260 ± 20 meV FWHM for both 20 and 100 eV impact energy. The results are compared to the H(2s) results of Misakian and Zorn.¹

\wedge
 wf
 The combined slow and fast fragment energy distribution at 100 eV impact energy is shown in Fig. 3 for both the red and blue wings. The red wing is slightly more intense, as shown in Fig. 1. The small difference in the energy distribution of the fast fragment distribution shape results from asymmetries in the pedestal line width in Fig. 1. Three peaks are observed in the distribution to be associated with either the blue or red wing. The strongest peak, near 80 meV and described above, arises from the slow atom distribution. The principal fast energy peak occurs at $(4 \pm 0.5$ eV). The minor secondary fast energy peak occurs at about $(2 \pm 0.5$ eV). The fast peak distribution is compared to H(2s) results from a number of authors. The results of Spezeski et al.⁴ are not shown on the plot but are nearly identical to those of Czuchlewski and Ryan.⁶ Our results for H(2p) lie between the work of Misakian and Zorn¹ and Leventhal et al.⁷ and indicate that the fast 2s and 2p atoms come from the same channels. A resolution of the fast H(2s) peak into two definite peaks at $(4.4 \pm 0.9$ eV and $2.3 (\pm 0.5$ eV) has only been reported by Leventhal et al. at an angle of 77° with respect to the electron beam axis. This result has been disputed by data of Spezeski et al., who pointed out that Misakian and Zorn did not find this double peak in their data. In addition, they pointed out the outstanding problem for the fast peak(s), which is: What other dissociating channels beside $Q_2(^1\Pi_u)$ autoionizing states that dissociate into $H(2p, 2s, 1s) + H(2p, 2s)$ contributed to this distribution? They concluded that other states contribute; and their main evidence was a model of the changing energy dependence of the H(2s) distribution function with electron impact energy. However accurate experimental excitation function studies were needed.

\wedge
 λ #
 wf
 We measured the accurate excitation function for the fast atom component. By placing the center of the bandpass of the spectrometer on the blue wing at 104 mÅ from line center and restricting the FWHM of the bandpass to 36 mÅ, we were able to obtain a data set that clearly shows the threshold for the fast processes. The excitation function for the blue wing is shown in Fig. 4. The first threshold is at 16.7 eV and must correspond to singly excited states tied to the $H(1s) + H(3p, 3s)$ dissociation limit. Cascade from Balmer- α contributes to the line profile above 16.67 eV. (The) other three thresholds can be traced to doubly excited states of H_2 which have the lowest $^2\Sigma_u^+$ and first excited $^2\Pi_u$ states

of H_2^+ as core orbitals. They are designated Q_1 and Q_2 , respectively. Fundamental calculations by Guberman¹⁷ allowed us to identify where the Q_1 and Q_2 states cross the right-hand edge of the Franck-Condon region. The most closely aligned thresholds of Guberman are associated with the measurement. In some cases more than one threshold lies within 0.5 eV of the measurement uncertainty. For the first time, dissociation along the $n=2$ asymptote is clearly identified as arising from a doubly excited state of H_2 at the lowest threshold of 23.0 eV. According to Guberman the Q_1 ($^1\Sigma_g^+(1)$) state is the responsible state. This same threshold has been found in other electron impact experiments: 1) dissociative excitation leading to $n=4$ product detected by Balmer- β radiation¹⁰, 2) dissociative excitation producing high Rydberg atoms studied by TOF techniques¹⁸, and 3) dissociative ionization processes producing H^+ ions measured by an ion mass spectrometer¹⁹. In all cases mentioned, perturbations from homogeneous interactions between the Q_1 ($^1\Sigma_g^+(1)$) state and the dissociating (e.g. $E, F^1\Sigma_g^+$ state for our case for $n=2$) or autoionizing state has lead to the same threshold. Non-adiabatic coupling of the first five $^1\Sigma_g^+$ states of H_2 has been recently treated on a *ab initio* basis by Wolniewicz and Dressler.²⁰

The next threshold is at 27.6 eV and can arise from Q_1 ($^1\Sigma_g^+(2)$) state at 27.2 eV, Q_1 ($^3,1\Pi_g(2)$) states at 27.4 eV and 27.5 eV, respectively, and/or Q_1 ($^3,1\Pi_u(2)$) states at 27.5 and 27.6 eV, respectively. However, the selection rules for molecular dissociation do not allow any Π_g transitions.²¹ The kinetic energy released by the allowed transitions to the higher-repulsive Q_1 states amount to approximately 6.5 eV per $H(2p)$ atom and contribute to the bump in the kinetic energy distribution between 6 and 8 eV. The final sharp threshold in Fig. 4 at 29.9 eV correlates with a set of Q_2 ($^1\Sigma_g^+, ^1,3\Pi_u$) states between 30 and 32 eV. The steep rise in cross section beginning at 30 eV confirms that the dominant contribution to the fast $H(2p)$ distribution arises from Q_2 ($^1\Sigma_g^+, ^1\Pi_u$) states as previously concluded for $H(2s)$.¹ Thus, many dissociation channels contribute to the fast atom dissociation process as predicted by Spezeski et al.⁴

CONCLUSIONS

Many new results can be gleaned from the $H\text{L}\alpha$ line profile measurement and the derived $H(2p)$ kinetic energy distribution. Our earlier result described the $H\text{L}\alpha$ dissociation cross-section budget at 100 eV.¹³ In brief, the low-resolution cross-section budget predicted that the partitioning of dissociation from singly excited states (slow atoms) and doubly excited states (fast atoms) occurred with fractional percentages of 0.73 and 0.27, respectively. Integrating under the kinetic energy distribution in Fig. 3 gives fractional percentages of 0.69 and 0.31, respectively. This verification testifies to the usefulness of the modified Born equation developed by this laboratory. The modified Born equation gives the absolute cross sections for each process. This slow/fast

atom quantum yield at 100 eV is quite different ^{from} ~~than~~ that found for H(2s) by Carnahan and Zipf.³ Their fractional percentage "0.87 and 0.13, respectively." ^{are}

The kinetic energy distribution of the fast H(2s) and H(2p) atoms appear to be identical from 2 to 10 eV. On the other hand, the slow-atom H(2p) distribution is different ^{from} ~~than~~ the H(2s) slow-atom distribution. Cascade from the higher Rydberg states contributes to approximately 6% of the slow-atom H(2p) signal at 100 eV. H(2s) contains less than 1% contribution from cascade at this energy.¹⁶ Both distributions are shown in Fig. 3 and have a high-energy cutoff near 1 eV. Ryan et al.⁵ pointed out that TOF techniques lose sensitivity as the energy approaches ~~to~~ zero. Based upon this, the difference is significant. uv techniques do not have a sensitivity problem at low energy.

ACKNOWLEDGMENTS

The research described in this text was carried out at the Jet Propulsion Laboratory, California Institute of Technology. The work was supported by the Air Force Office of Scientific Research (AFOSR), the Aeronomy Program of the National Science Foundation Program (grant ATM-9320589) and NASA Planetary Atmospheres, Astronomy/Astrophysics and Space Physics Program Offices. S. M. Ahmed and R. Multari were each supported by a National Research Council Resident Research Associateship.

REFERENCES

- ¹M. Misakian and J. C. Zorn, Phys. Rev. A 6, 2180 (1972).
- ²R. Clappitt, Phys. Lett. 28A, 581 (1969).
- ³B. L. Carnahan and E. C. Zipf, Phys. Rev. A 16, 991 (1977).
- ⁴J. J. Spezeski, O. F. Kalman and L. C. McCyntyre, Phys. Rev. A 22, 1906 (1980).
- ⁵S. R. Ryan, J. J. Spezeski, O. F. Kalman, W. E. Lamb, L. C. McCyntyre and W. H. Wing, Phys. Rev. A 19, 2192 (1979).
- ⁶S. J. Czuchlewski and S. R. Ryan, Bull. Am. Phys. Soc. 18, 688 (1973).
- ⁷M. Leventhal, R. T. Robiscoe and K. R. Lea, Phys. Rev. 158, 49 (1967).
- ⁸J. A. Beswick and M. Glaa-Maujean, Phys. Rev. A 35, 3339 (1987).
- ⁹T. Ogawa and M. Higo, Chem. Phys. Lett. 65, 610 (1979).
- ¹⁰T. Ogawa and M. Higo, Chem. Phys. 52, 55 (1980).
- ¹¹K. Nakashima, M. Tanguchi, and T. Ogawa, Chem. Phys. Lett. 197, 72 (1992).
- ¹²T. Ogawa, S. Ihara, and K. Nakahima, Chem. Phys. 161, 509 (1992).
- ¹³J. M. Ajello, D. E. Shemansky, and G. K. James, Ap. J. 371, 422 (1991).

⁴X. Liu, S. M. Ahmed, R. Multari, G. K. James, and J. M. Ajello, 'High Resolution Electron Impact Spectrum of Molecular Hydrogen', Ap. J. Supp., In Press (1995).

¹⁵R. J. Van Brunt and R.N. Zare, J. Chem. Phys. 48, 4304 (1968)

¹⁶W. H. Press, B. P. Flannery, S. A. Teukolsky, and W. T. Vetterling, *Numerical Recipes* (Cambridge University Press, Cambridge, England, 1987).

¹⁷S. L. Guberman, J. Chem. Phys. 78, 1404 (1983).

¹⁸J. A. Schiavone, K. C. Smyth, and R. S. Freund, J. Chem. Phys. 63, 1043 (1975).

¹⁹A. Crowe and J. W. McConkey, Phys. Rev. Lett. **31**, 192 (1973).

²⁰L. Wolniewicz and K. Dressier, J. Chem. Phys. 100, 444 (1994).

"G. H. Dunn, Phys. Rev. Lett. 8, 62 (1963).

"D. E. Shemansky, J. M. Ajello, D. T. Hall, and B. Franklin, Ap. J. **296**, 774 (1985).

TABLE OF FIGURES

FIGURE 1. Overplot of 20 eV and 100 eV H L α line profiles compared to the instrument slit function. The line profiles were measured in third order and the slit function was measured at zero order. The operating conditions were established as follows: (1) background gas pressure of 10^{-4} torr and (2) electron beam current of 269 μ A. The data statistics were better than 1%. The wavelength step size was 2.667 mÅ. The FWHM of the H L α features at 100 eV and 20 eV and the instrument slit function are 47 mÅ, 49 mÅ, and 24 mÅ, respectively,

FIGURE 2. Kinetic energy H(2p) distribution of slow atoms at both 20 and 100 eV compared to work of Misakian and Zorn.¹

Figure 3. Combined slow and fast H(2p) atom distribution function compared to published results for fast H(2s) atoms.

Figure 4. Optical excitation function of H L α line blue wing. The uv bandpass (36 mÅ FWHM) is offset by 104 mÅ from the line center. The channel spacing is 200 meV. The electron gun energy resolution is 300 meV. The energy scale was calibrated from the 14.68 eV AP of line center.

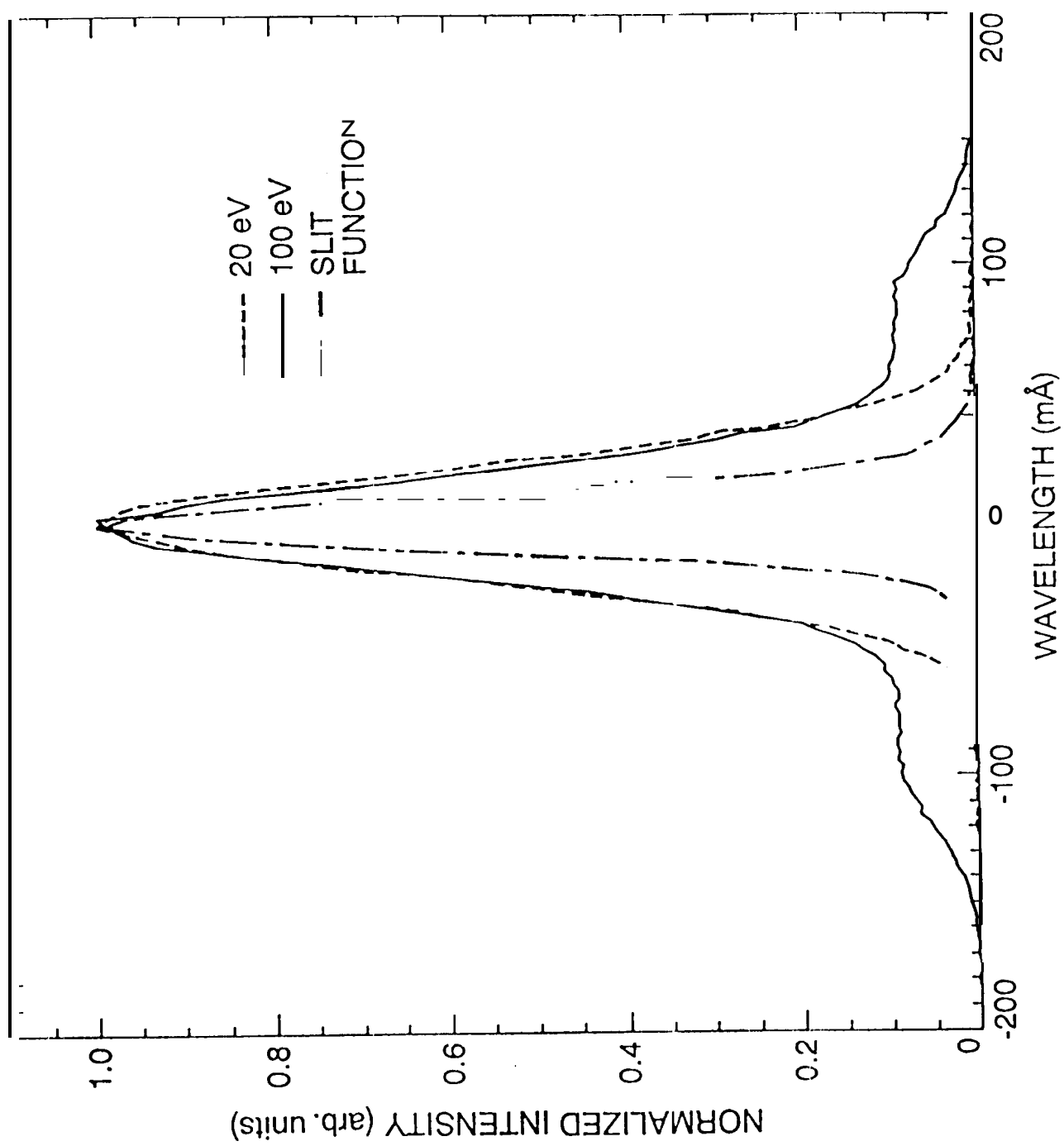


Fig. 1

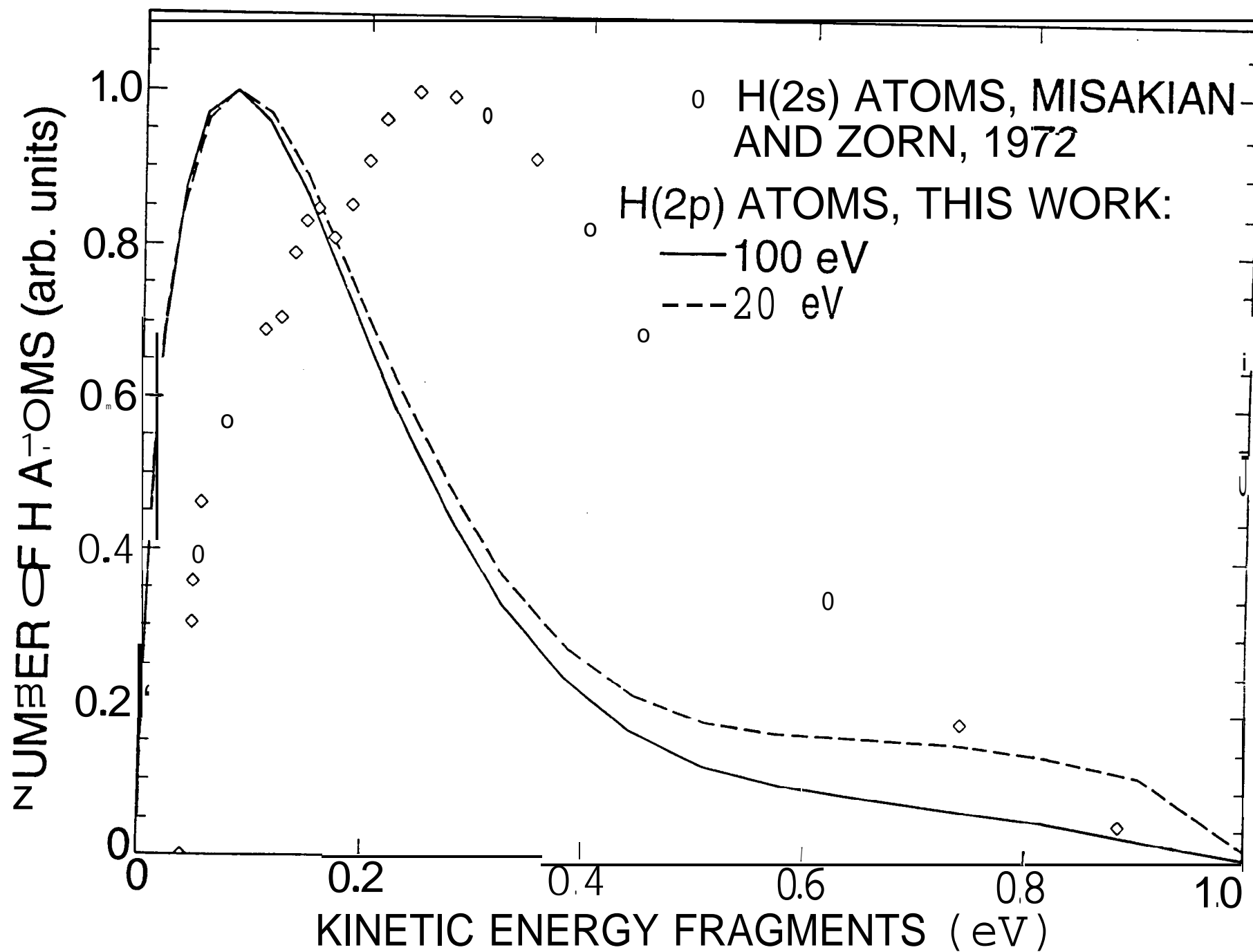


Fig. 2

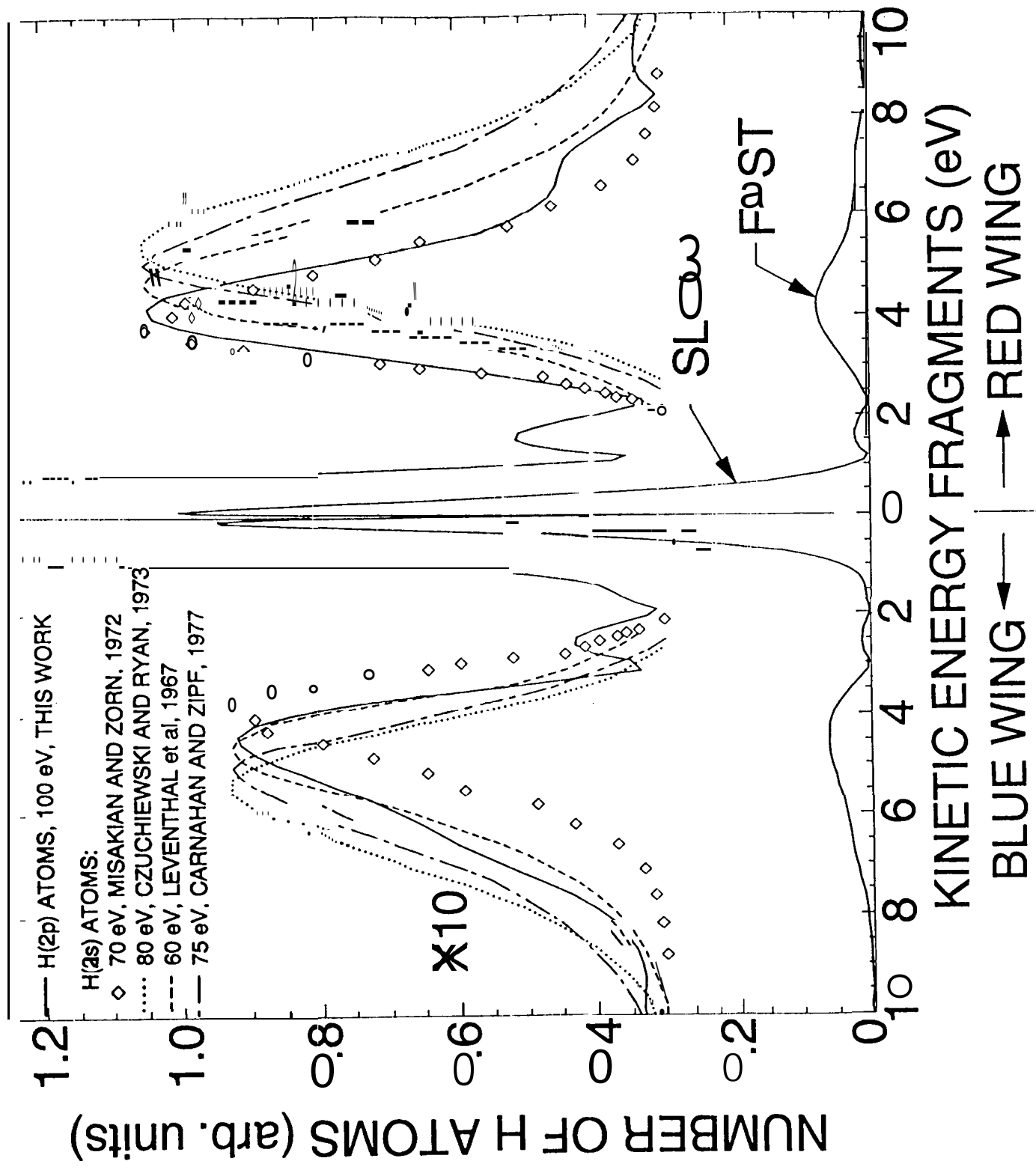


Fig. 3

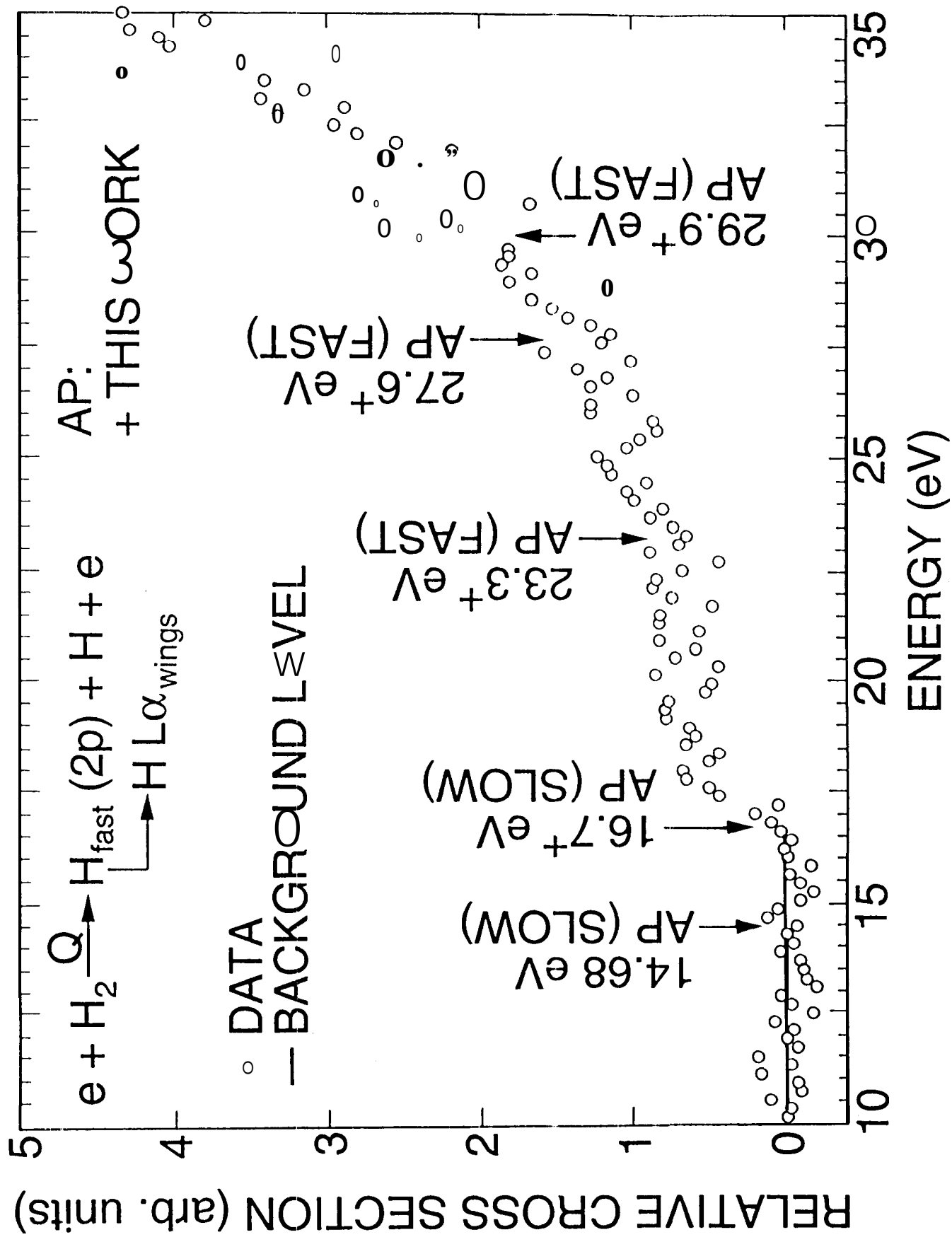


Fig. 4